

Protective effect of magnesium acetyltaurate and taurine against NMDA-induced retinal damage involves reduced nitrosative stress

Azliana Jusnida Ahmad Jafri,¹ Renu Agarwal,¹ Igor Iezhitsa,^{1,2} Puneet Agarwal,³ Alexander Spasov,² Alexander Ozerov,² Nafeeza Mohd Ismail¹

¹Center for Neuroscience Research, Faculty of Medicine, Universiti Teknologi MARA Sungai Buloh Campus, Selangor, Malaysia;

²Volgograd State Medical University, Research Institute of Pharmacology, Volgograd, Russia; ³Faculty of Medicine, International Medical University, IMU Clinical School, Seremban, Malaysia

Purpose: Retinal nitrosative stress associated with altered expression of nitric oxide synthases (NOS) plays an important role in excitotoxic retinal ganglion cell loss in glaucoma. The present study evaluated the effects of magnesium acetyltaurate (MgAT) on changes induced by N-methyl-D-aspartate (NMDA) in the retinal expression of three NOS isoforms, retinal 3-nitrotyrosine (3-NT) levels, and the extent of retinal cell apoptosis in rats. Effects of MgAT with taurine (TAU) alone were compared to understand the benefits of a combined salt of Mg and TAU.

Methods: Excitotoxic retinal injury was induced with intravitreal injection of NMDA in Sprague-Dawley rats. All treatments were given as pre-, co-, and post-treatment with NMDA. Seven days post-injection, the retinas were processed for measurement of the expression of NOS isoforms using immunostaining and enzyme-linked immunosorbent assay (ELISA), retinal 3-NT content using ELISA, retinal histopathological changes using hematoxylin and eosin (H&E) staining, and retinal cell apoptosis using terminal deoxynucleotidyl transferase-mediated dUTP nick end-labeling (TUNEL) staining.

Results: As observed on immunohistochemistry, the treatment with NMDA caused a 4.53-fold increase in retinal nNOS expression compared to the PBS-treated rats ($p < 0.001$). Among the MgAT-treated groups, only the pretreatment group showed significantly lower nNOS expression than the NMDA-treated group with a 2.00-fold reduction ($p < 0.001$). Among the TAU-treated groups, the pre- and cotreatment groups showed 1.84- and 1.71-fold reduction in nNOS expression compared to the NMDA-treated group ($p < 0.001$), respectively, but remained higher compared to the PBS-treated group ($p < 0.01$). Similarly, iNOS expression in the NMDA-treated group was significantly greater than that for the PBS-treated group (2.68-fold; $p < 0.001$). All MgAT treatment groups showed significantly lower iNOS expression than the NMDA-treated groups (3.58-, 1.51-, and 1.65-folds, respectively). However, in the MgAT co- and post-treatment groups, iNOS expression was significantly greater than in the PBS-treated group (1.77- and 1.62-folds, respectively). Pretreatment with MgAT caused 1.77-fold lower iNOS expression compared to pretreatment with TAU ($p < 0.05$). In contrast, eNOS expression was 1.63-fold higher in the PBS-treated group than in the NMDA-treated group ($p < 0.001$). Among all treatment groups, only pretreatment with MgAT caused restoration of retinal eNOS expression with a 1.39-fold difference from the NMDA-treated group ($p < 0.05$). eNOS expression in the MgAT pretreatment group was also 1.34-fold higher than in the TAU pretreatment group ($p < 0.05$). The retinal NOS expression as measured with ELISA was in accordance with that estimated with immunohistochemistry. Accordingly, among the MgAT treatment groups, only the pretreated group showed 1.47-fold lower retinal 3-NT than the NMDA-treated group, and the difference was significant ($p < 0.001$). The H&E-stained retinal sections in all treatment groups showed statistically significantly greater numbers of retinal cell nuclei than the NMDA-treated group in the inner retina. However, the ganglion cell layer thickness in the TAU pretreatment group remained 1.23-fold lower than that in the MgAT pretreatment group ($p < 0.05$). In line with this observation, the number of apoptotic cells as observed after TUNEL staining was 1.69-fold higher after pretreatment with TAU compared to pretreatment with MgAT ($p < 0.01$).

Conclusions: MgAT and TAU, particularly with pretreatment, reduce retinal cell apoptosis by reducing retinal nitrosative stress. Pretreatment with MgAT caused greater improvement in NMDA-induced changes in iNOS and eNOS expression and retinal 3-NT levels than pretreatment with TAU. The greater reduction in retinal nitrosative stress after pretreatment with MgAT was associated with lower retinal cell apoptosis and greater preservation of the ganglion cell layer thickness compared to pretreatment with TAU.

Excitotoxicity caused by glutamate through

N-methyl-D-aspartate (NMDA) receptors is believed to play an important role in the neuronal loss in glaucomatous neuropathy. To understand the pathophysiology of glaucoma, which is characterized by loss of retinal ganglion cells (RGCs), mechanical and vascular theories have been proposed. Both theories have considerable overlap, and the

Correspondence to: Renu Agarwal, Center for Neuroscience Research, Faculty of Medicine, Universiti Teknologi MARA Sungai Buloh Campus, Selangor, Malaysia; Phone:+60361265000; email: renuag02@gmail.com

component of excitotoxicity is compatible with both [1]. Although the vitreous levels of glutamate were not found to be elevated in patients with glaucoma [2], a definitive role of glutamate-mediated excitotoxicity in glaucomatous neuropathy is widely accepted [3,4]. Excitotoxicity involves loss of ionic homeostasis that sets in a self-reinforcing cascade of events finally culminating in cell death. Initial depolarization involves α -amino-3-hydroxy-5-methyl-4-isoxazolepropionic acid (AMPA) receptors, and subsequent activation of NMDA receptors leads to influx of Na^+ and Ca^{2+} [4]. Increase in intracellular Ca^{2+} is particularly significant as it has several deleterious consequences, such as activation of proteases, nucleases, and lipases, production of free radicals, and mitochondrial injury, that sets in a self-escalating cascade leading to cell death [5]. Tymianski et al. showed that NMDA receptors are particularly efficient in initiating Ca^{2+} influx-associated apoptotic signaling [6]. Increased Ca^{2+} influx as a result of NMDA stimulation causes activation of Ca^{2+} -dependent nitric oxide synthases (NOS), neuronal NOS (nNOS), and endothelial NOS (eNOS) [7,8]. NMDA also stimulates inducible NOS (iNOS) expression, and this occurs in a Ca^{2+} independent manner [9,10]. NOS activation causes increased NO production and formation of the nitrogen free radical, peroxynitrite (ONOO^-). This nitrogen free radical triggers neuronal injury and apoptosis [11,12]. Neufeld et al. demonstrated the presence of all three isoforms of NOS in the optic nerve head of eyes with primary open angle glaucoma [13]. The nNOS and iNOS expression was increased in astrocytes of the lamina cribrosa suggesting the presence of excessive levels of NO in the glaucomatous optic nerve head, which may be neurodestructive, locally, to the RGC axons.

Considering the prominent role of NMDA receptors in apoptotic loss of retinal cells, animal models with NMDA-induced retinal cell injury have been widely investigated and used for glaucoma-related investigations [14-16]. Lam et al. showed that intravitreal injection of NMDA in adult albino Lewis rats results in loss of inner retinal elements [17]. In other studies, antagonism of NMDA receptors was shown to protect against NMDA-induced retinal cell loss [18-20]. Magnesium (Mg), a calcium antagonist, is known to antagonize NMDA-mediated excitotoxicity [21]. Mg also inhibits elevated NOS activity in endothelial cells and neurons [22,23]. Studies have also shown that taurine (TAU) has the ability to directly interact with NMDA receptors [24] and attenuate the effects of overactive NMDA receptors [25]. TAU protects neurons by inhibiting glutamate-induced increase in intracellular calcium [26-28]. Previous studies have shown that TAU reduces nNOS expression in high-glucose exposed Schwann cells and activated C6 glioma cells [29,30]. TAU is a naturally occurring sulfonic acid derived from cysteine. It is the most

abundant amino acid found in mammals and is widely distributed in animal tissues, especially nervous tissue and the retina [31]. TAU deficiency was shown to cause loss of RGCs along with cone photoreceptors in mouse [32]. Similarly, another study showed that TAU deficiency causes retinal damage as indicated by morphological and electroretinogram changes while infusion of TAU protects against retinal damage [33]. In previous studies, we found that magnesium acetyltaurate (MgAT), a salt consisting of Mg and TAU, protects against endothelin-1 and NMDA induced retinal damage [34,35]. However, it remains unknown whether this effect of MgAT involves altered retinal NOS expression. Moreover, it is not clear whether the addition of Mg to TAU has greater effectiveness than TAU alone. Therefore, we performed the present study to evaluate whether the protective effect of MgAT against NMDA-induced retinal damage involves altered NOS expression and reduction in nitrosative stress. Second, we investigated the similar effect of TAU alone in comparison with MgAT to determine whether the addition of Mg to TAU provides greater retinal cell protection compared to TAU alone.

METHODS

All experimental protocols and procedures in this study followed the tenets of the Association for Research in Vision and Ophthalmology (ARVO) Statement for the Use of Animals in Ophthalmic and Vision Research. The study was approved by Animal Care and Use Committee of Universiti Teknologi MARA. Sprague Dawley rats weighing 220–250 g, of either sex, were procured from the Laboratory Animal Care Unit, Faculty of Medicine, Universiti Teknologi Mara. The rats were housed under standard laboratory conditions with a 12 h:12 h light-dark cycle with access to food and water ad libitum. All animals were subjected to general and ophthalmic examination, and those found to be normal were included in this study. NMDA and TAU were purchased from Sigma-Aldrich (St. Louis, MO). MgAT was synthesized at the Chemical Pharmaceutical Department of the Research Institute of Pharmacology (Volograd State Medical University, Volograd, Russian Federation) as described previously [36].

Study design: The Sprague Dawley rats were randomly divided into eight groups of 24 rats each ($n=48$ eyes per group). Groups 1 and 2 were intravitreally injected with PBS (1X; 1 mM KH_2PO_4 , 155 mM NaCl , 2 mM $\text{Na}_2\text{HPO}_4 \cdot 7\text{H}_2\text{O}$, pH 7.4) and 160 nM of NMDA, respectively. Group 3 received an intravitreal injection of 320 nM of MgAT, 24 h before 160 nM of NMDA (the MgAT pretreatment group). Rats in group 4 were injected with 160 nM of NMDA and 320 nM of MgAT simultaneously (the MgAT cotreatment

group). Group 5 was injected with 160 nM of NMDA, 24 h before 320 nM of MgAT (the MgAT post-treatment group). Selection of the dose of NMDA and MgAT was based on our previous studies [35,37]. Groups 6, 7, and 8 similarly received 320 nM of TAU, a concentration equimolar to MgAT, as pre-, co-, and post-treatment with NMDA, respectively. Seven days after intravitreal injection, the animals were euthanized with an intraperitoneal injection of pentobarbital (100 mg/kg). A suture was placed at the 12 o'clock position for better orientation, and both eyes were enucleated and processed for immunohistochemical examination of NOS expression (n=6 for each NOS isoform), enzyme-linked immunosorbent assay (ELISA) for quantitative estimation of NOS expression (n=6 for each NOS isoform), estimation of retinal nitrosative stress using ELISA (n=6), histological examination of retinal morphology (n=6), and estimation of the extent of retinal cell apoptosis using terminal deoxynucleotidyl transferase-mediated dUTP nick end-labeling (TUNEL) staining (n=6). For estimation of NOS expression using ELISA, retinas from two eyes of the same animal were pooled. The six eyes for the estimation of each of the remaining parameters were from six different animals. For the histological and immunohistological examinations, the paraffin-embedded tissue was sectioned at 1 mm from the temporal edge of the optic nerve head. For measurements, images of the retinal sections were captured from three randomly selected areas using a digital camera attached to a light microscope at 20X magnification (NIS-Elements Basic Research, Nikon Instrument Inc, New York, NY). All estimations were performed by two masked observers. For each observer, the average of the values from three random areas was calculated, and subsequently, the average of the values obtained by two observers was taken as the final estimate.

For the intravitreal injections, the rats were anesthetized with an intraperitoneal injection of sodium pentobarbital (65 mg/kg) followed by a drop of 0.5% Alcaine (Sigma) on the ocular surface for local anesthesia. First, a 30-gauge needle was used to puncture the sclera superonasally 1 mm behind the limbus. This was followed by insertion of a 10 µl Hamilton syringe through the puncture site, and the injections were made using the Hamilton syringe. All injections were given in a total volume of 2 µl slowly over 1 min to avoid any pressure-induced retinal damage.

Immunohistochemical staining for NOS isoforms: For immunohistochemical staining, the tissue sections were placed on a poly-L-lysine glass slide. Antigen retrieval was done using 10 mM of Tween-200 (pH 6.0) at the boiling point for 20 min in a domestic microwave oven. Then, the slides were washed in running cold tap water for 10 min. After that, the slides

were washed twice with TBS plus 0.025% Triton X-100 for 5 min each followed by peroxidase blocking for 30 min and washing with TBS plus Triton X-100 0.025% for 5 min. The primary antibodies used were monoclonal rabbit antibody for nNOS, iNOS 2 and eNOS (Santa Cruz Biotechnology, CA) while the secondary antibody was anti-rabbit conjugated with fluorescein isothiocyanate (FITC). For treatment with the primary antibody, 100 µl was diluted with 10 mM Tris 1% bovine serum albumin (BSA; 2:98), and incubation was done overnight at 4 °C. Following day, the slides were rinsed with TBS 0.025% Triton X-100 for 5 min. Then, the sections were incubated with the secondary antibody for 1 h. After the incubation period, the slides were washed twice with TBS plus 0.025% Triton X-100 for 5 min each and counter-stained with 4',6-diamidino-2-phenylindole (DAPI) diluted in PBS 1 mM (1:999) for 10 min. The slides were then mounted and observed using a fluorescence microscope (Olympus; BX61TRF-FL-CCD) in a dark room at an excitation 488/520 nm filter for FITC and 358 nm for DAPI. Three randomly selected fields measured from each section were viewed at 20X magnification. Images were saved in the .jpg image format, the number of fluorescent signals in the inner retina (IR) was counted in the field of view, and the average from three areas in each section was obtained. Subsequently, the number of fluorescent signals per 100 µm² area of the IR was calculated. The average numeric values obtained by two masked investigators were taken as the final estimate and used for the statistical analysis.

ELISA for quantitative estimation of NOS isoforms: The retinal expression of all three NOS isoforms was quantified using commercially available ELISA kits (Elabscience Biotechnology, Houston, TX) according to the manufacturer's protocol. Briefly, the retinal tissues were homogenized in 500 µl of PBS on ice and centrifuged to get the supernatant. Then, the standards and the samples were added to the designated wells in plates precoated with antibodies (nNOS, iNOS and eNOS). After incubation for 90 min, the biotinylated detection antibody and the horseradish peroxidase (HRP) conjugate were added. The plates were washed, and the substrate reagent was added in a dark room. The reactions were stopped with the stop solution, and optical density was measured at the 450 nm wavelength. All estimations were done in duplicate. The total protein content in the retinal samples was estimated using the Bradford method.

ELISA for estimation of retinal nitrosative stress: The measurement of 3-nitrotyrosine (3-NT) indirectly provides estimation of peroxynitrite in the samples. For the nitrotyrosine assay, the retinal tissue was homogenized on ice in 100 µl of PBS and centrifuged to get the supernatant. The assay was

performed according to the manufacturer's instructions using an ELISA kit (Elabscience Biotechnology, Houston, TX). All estimations were performed in duplicate.

Histological examination of retinal morphology: Morphology of the retina was examined using hematoxylin and eosin (H&E) staining. The enucleated eyes were fixed in 10% formaldehyde for 24 h. The anterior segments were carefully removed, and the rest of the eyecups were embedded in paraffin and sectioned at 3 μm thickness at 1 mm from the temporal edge of the optic disc. The sections were stained with H&E and examined under a light microscope. Three randomly selected fields of view from each section were calibrated at 20X magnification and saved in the .jpg image format. Using image analysis software (ImageJ 1.31, National Institutes of Health, Bethesda, MD), we estimated the thickness of the ganglion cell layer (GCL), the thickness of the IR comprising the GCL and the inner plexiform layer (IPL), and the number of retinal cell nuclei in the area of the IR. The parameters used for morphometric analysis included the fractional thickness of the GCL within the IR and the number of nuclei per 100 μm^2 of the IR. Cell nuclei with a diameter of less than 7 μm and those of morphologically distinguishable glial cells and vascular endothelial cells were excluded from the cell count [38-40]. All observations were made by two masked investigators. The average of the numeric values obtained by two masked investigators was taken as the final estimate.

TUNEL for detection of apoptotic retinal cells: Detection of DNA fragmentation in apoptotic retinal cells was done with TUNEL staining. We used the In situ DNA Fragmentation Assay Kit (Biovision Inc, Milpitas, CA) according to the manufacturer's protocol. The tissue sections were placed in an incubator at 60 °C for 30 min, and the paraffin was removed with xylene. This was followed by rehydration and fixation in 4% formaldehyde. Antigen retrieval was performed with 100 μl of Proteinase K (2 μl Protease K + 998 μl Tris-HCl, pH 8, 50 mM EDTA) for 5 min. The sections were then incubated with 50 μl of DNA labeling solution (TdT reaction buffer:TdT enzyme:Br-dUTP) in a dark humidified chamber for 60 min. Following this, the sections were incubated with anti-BrdU FITC antibody for 30 min at room temperature, and further incubation was done for 30 min in a dark humidified chamber with 100 μl of propidium iodide. After mounting, the sections were viewed immediately using FITC (488/520 nm) and rhodamine (488/623 nm) filters. Apoptotic cells exhibited strong green fluorescence whereas other cells showed strong red counterstaining. Images were captured using an Olympus BX5 Fluorescence Trinocular Microscope (Olympus, Tokyo, Japan) at 20X magnification and saved as .jpg images. The

apoptotic signals in three randomly selected areas of IR per section were counted by two masked investigators. The average of the numeric values obtained by the two masked investigators was taken as the final estimate.

Statistical analysis: All values were expressed as mean \pm standard deviation (SD). Statistical comparison among groups was performed using one-way ANOVA with Bonferroni's correction. A p value of less than 0.05 was considered statistically significant.

RESULTS

Effect of MgAT and TAU on NMDA-induced changes in retinal NOS expression: Immunohistochemistry: The changes in the expression of nNOS in response to treatment with MgAT or TAU were estimated by comparing the number of nNOS-positive cells per 100 μm^2 of the IR among the groups. We observed the significantly greater presence of nNOS in the IR of NMDA-treated group whereas minimal fluorescence was observed for nNOS in the PBS and MgAT pretreatment groups. The number of immunopositive cells for nNOS was 0.044 ± 0.009 in the NMDA-treated group compared to 0.01 ± 0.001 and 0.022 ± 0.006 in the PBS- and MgAT-pretreated groups, respectively ($p < 0.001$ for both groups). In the MgAT cotreatment group, although nNOS expression was significantly lower than in the NMDA-treated group with mean values of 0.030 ± 0.008 ($p < 0.01$), the expression remained significantly higher than that in the PBS-injected group ($p < 0.05$). Among the TAU-treated groups, the number of nNOS-positive cells in the pre- and cotreatment groups was 0.024 ± 0.005 and 0.028 ± 0.003 , which was significantly lower than that in the NMDA-treated group ($p < 0.001$) but remained significantly higher than that in the PBS-injected group ($p < 0.01$). nNOS expression in the MgAT and TAU post-treatment groups showed a mean value of 0.034 ± 0.006 and 0.036 ± 0.003 , respectively. In both groups, the nNOS expression was significantly greater compared to that in the PBS-treated group ($p < 0.001$) and was comparable to that in the NMDA-treated group ($p > 0.05$; Figure 1A,B).

Expression of iNOS, which was also expressed as iNOS-positive cells/100 μm^2 of the IR, showed a trend similar to that for nNOS with significantly greater expression in the NMDA-treated group with a mean value of 0.057 ± 0.005 compared to 0.021 ± 0.004 in the PBS-treated group ($p < 0.001$). In the MgAT pre-, co-, and post-treatment groups, the mean iNOS-positive cell numbers were 0.016 ± 0.003 , 0.037 ± 0.005 , and 0.034 ± 0.005 , respectively. In all three MgAT-treated groups, iNOS expression was significantly lower compared to that in the NMDA-treated group ($p < 0.001$ for all three groups). However, only in the pretreatment group, the level

of iNOS expression was comparable to that in the PBS-treated group ($p > 0.05$). Among the TAU-treated groups, the pre- and cotreatment groups showed significantly lower iNOS expression compared to the NMDA-treated group with a mean immunopositive cell count of 0.028 ± 0.005 and 0.044 ± 0.012 , respectively ($p < 0.001$ and $p < 0.01$, respectively). Although the TAU pretreatment group showed no significant difference from the PBS-treated group, iNOS expression in this group was statistically significantly greater than that in the MgAT pretreatment group ($p < 0.05$). In the TAU post-treatment group, iNOS expression was significantly greater than that in the PBS-treated group ($p < 0.001$) with a mean value of 0.039 ± 0.005 (Figure 2A,B).

To estimate the changes in the expression of eNOS, the number of eNOS-positive cells/ $100 \mu\text{m}^2$ of the IR was compared among the groups. In contrast to nNOS and iNOS, we observed significantly lower eNOS expression in the NMDA-treated group with a mean immunopositive cell count of 0.032 ± 0.006 compared to 0.052 ± 0.008 in the PBS-treated group ($p < 0.001$). Among all treatment groups, only

the MgAT pretreatment group showed significantly greater eNOS expression with a mean immunopositive cell count of 0.045 ± 0.004 compared to that in the NMDA-treated group ($p < 0.05$). In the MgAT co- and post-treatment groups, eNOS expression was 0.037 ± 0.001 and 0.037 ± 0.004 , respectively ($p < 0.01$ versus PBS-treated group). The eNOS expression in the TAU pre-, co-, and post-treatment groups was significantly lower than that in the PBS-treated group ($p < 0.001$, $p < 0.001$, and $p < 0.01$, respectively) with mean values of 0.033 ± 0.006 , 0.036 ± 0.003 , and 0.037 ± 0.005 , respectively (Figure 3A,B). Furthermore, eNOS expression in the MgAT pretreatment group was significantly lower than that in the corresponding TAU-treated group ($p < 0.05$; Figure 3A,B).

Effect of MgAT and TAU on NMDA-induced changes in retinal NOS expression: ELISA: We further confirmed the effects of treatment with MgAT and TAU on retinal expression of NOS isoforms using ELISA (Table 1). The expression of nNOS increased by 139-fold after intravitreal injection of NMDA compared to that in the PBS-injected group ($p < 0.001$). Pretreatment with MgAT and TAU resulted in 11.21- and

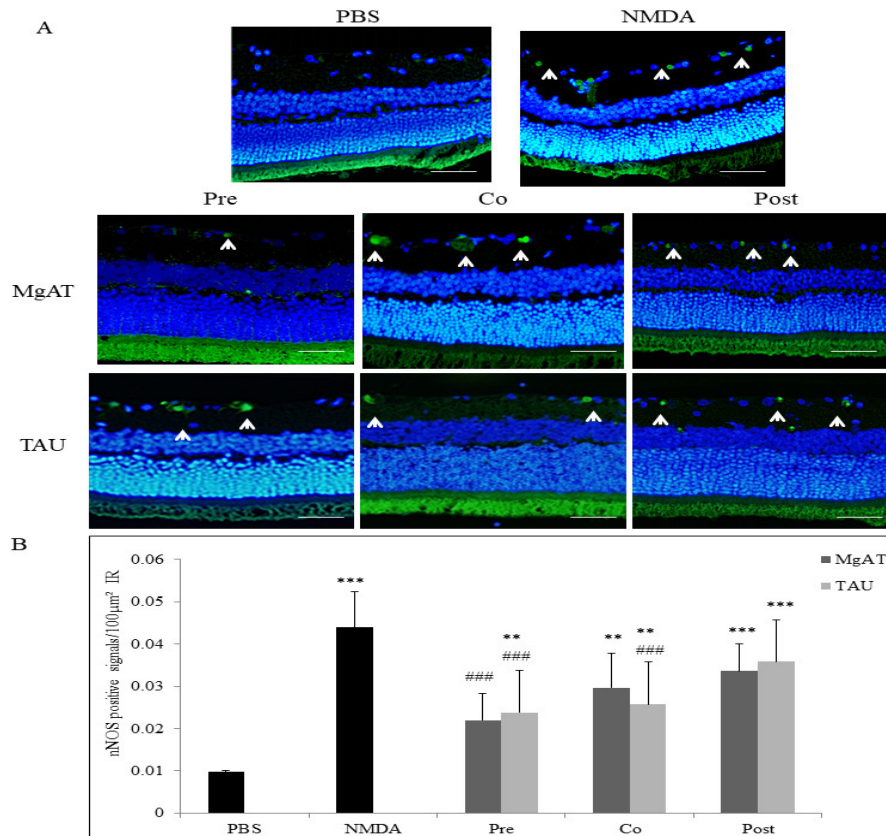


Figure 1. Effect of MgAT and TAU on NMDA-induced changes in nNOS expression. A: Microphotographs of retinal sections immunostained with nNOS antibodies showing the effect of MgAT and TAU on the NMDA-induced increase in the expression of nNOS. (20X). Green fluorescence shows nNOS expression stained with fluorescein isothiocyanate (FITC; shown by arrow) while blue fluorescence shows retinal nuclei stained with 4',6-diamidino-2-phenylindole (DAPI). Scale bar represents $50 \mu\text{m}$. B: Quantitative estimation of the effect of MgAT and TAU on the NMDA-induced increase in the expression of nNOS is also represented graphically. Pre, Co, and Post indicate that MgAT/TAU were injected 24 h before, simultaneously, or 24 h after intravitreal administration of NMDA, respectively. * $p < 0.05$ versus the PBS-treated group, ** $p < 0.01$ versus the PBS-treated group, *** $p < 0.001$

versus the PBS-treated group, ### $p < 0.001$ versus the NMDA-treated group, $n = 6$; bars represent mean \pm SD. NMDA: N-methyl-D-aspartic acid, MgAT: Magnesium acetyl taurate, TAU: Taurine, GCL: Ganglion cell layer.

9.22-fold reduction, respectively, compared to the NMDA-treated group ($p < 0.01$). In the MgAT and TAU pretreated groups, nNOS expression remained significantly higher than in the PBS-treated group ($p < 0.05$ and $p < 0.001$, respectively). In the MgAT and TAU cotreatment groups, nNOS expression remained significantly greater than in the PBS-treated group ($p < 0.05$ and $p < 0.001$, respectively). However, nNOS expression was significantly lower than in the NMDA-treated group ($p < 0.05$). Post-treatment with MgAT and TAU did not cause a significant change in retinal nNOS expression compared to the NMDA-treated group and remained significantly greater than in the PBS-treated group ($p < 0.05$ and $p < 0.01$, respectively).

iNOS expression in NMDA-exposed retinas increased by 111.65-fold compared to the PBS-exposed retinas ($p < 0.001$). Pretreatment with MgAT and TAU resulted in a 32.55- and 4.85-fold reduction in NMDA-induced retinal iNOS expression ($p < 0.01$). However, it remained significantly greater than the PBS-injected group ($p < 0.05$ and $p < 0.01$, respectively). Moreover, the iNOS expression in the MgAT-pretreated group was significantly lower than in the TAU pretreatment group ($p < 0.01$). Cotreatment with MgAT and TAU, however,

resulted in reduction of NMDA-induced iNOS expression by 5.37- and 3.72-fold, respectively, ($p < 0.01$). iNOS expression in both of these groups, compared to the PBS-treated group, remained 20.81- ($p < 0.01$) and 30.01-fold ($p < 0.001$) higher, respectively. Similarly in the MgAT and TAU post-treatment groups, retinal iNOS expression was significantly lower than in the NMDA-treated group ($p < 0.05$) but remained significantly greater than in the PBS-treated group ($p < 0.05$ and $p < 0.01$ respectively).

In contrast to nNOS and iNOS, retinal eNOS expression was 2.76-fold lower in the NMDA-treated group compared to the PBS-treated group ($p < 0.01$). Pretreatment with MgAT caused a 1.97-fold increase in retinal eNOS expression compared to the NMDA-treated group ($p < 0.05$). Pretreatment with TAU, however, did not cause a significant increase in eNOS expression compared to the NMDA-treated group and remained significantly lower than that of the MgAT-pretreated group ($p < 0.05$). In the MgAT and TAU cotreatment groups, eNOS expression was significantly lower than in the PBS-treated group ($p < 0.05$); however, in the MgAT-pretreated group, eNOS expression was 1.64-fold greater than in the NMDA-treated group ($p < 0.05$). Both post-treatment groups

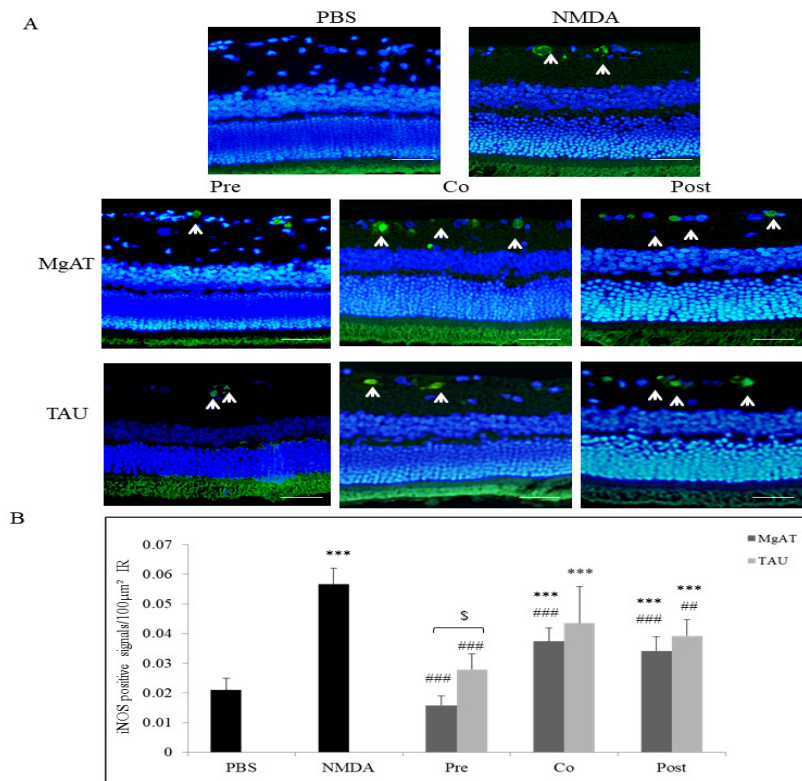


Figure 2. Effect of MgAT and TAU on NMDA-induced changes in iNOS expression. **A:** Microphotographs of retinal sections immunostained with iNOS antibodies showing the effect of MgAT and TAU on the NMDA-induced increase in the expression of iNOS (20X). Green fluorescence shows iNOS expression stained with FITC (shown by arrow) while blue fluorescence shows retinal nuclei stained with 4',6-diamidino-2-phenylindole (DAPI). Scale bar represents 50 μm . **B:** Quantitative estimation of the effect of MgAT and TAU on the NMDA-induced increase in the expression of iNOS is also represented graphically. Pre, Co, and Post indicate that MgAT/TAU were injected 24 h before, simultaneously, or 24 h after intravitreal administration of NMDA, respectively. *** $p < 0.001$ versus the PBS-treated group, ## $p < 0.01$

versus the NMDA-treated group, ### $p < 0.001$ versus the NMDA-treated group, \$ $p < 0.05$ corresponding MgAT versus TAU groups, $n = 6$; bars represent mean \pm SD. NMDA: N-methyl-D-aspartic acid, MgAT: Magnesium acetyl taurate, TAU: Taurine, GCL: Ganglion cell layer.

showed significantly lower eNOS expression compared to the PBS-treated group ($p < 0.05$), and no difference compared to the NMDA-treated group was observed.

Effect of MgAT and TAU on NMDA-induced retinal 3-NT contents: Retinal nitrosative stress was evaluated by measuring the retinal 3-NT levels. The NMDA-treated group showed significantly higher 3-NT levels compared to the PBS-treated group with a 1.61-fold increase ($p < 0.001$). Among the MgAT treatment groups, only the pretreated group showed a 1.47-fold lower retinal 3-NT level compared to the NMDA-treated group, and the difference was significant ($p < 0.001$).

None of the TAU-treated groups showed significantly lower retinal 3-NT levels compared to the NMDA-treated group. Moreover, in the TAU pretreatment group, the 3-NT level was 1.38-fold greater than in the MgAT pretreatment group ($p < 0.01$; Table 2).

Effect of MgAT and TAU on NMDA-induced changes in retinal morphology: Examination of the H&E-stained retinal sections showed that the fraction of GCL thickness within the IR was 24.75 ± 1.850 in the NMDA-injected rat eyes compared to 39.18 ± 4.200 in the PBS-treated group, amounting to a 1.58-fold reduction ($p < 0.001$). In the MgAT pre- and cotreatment

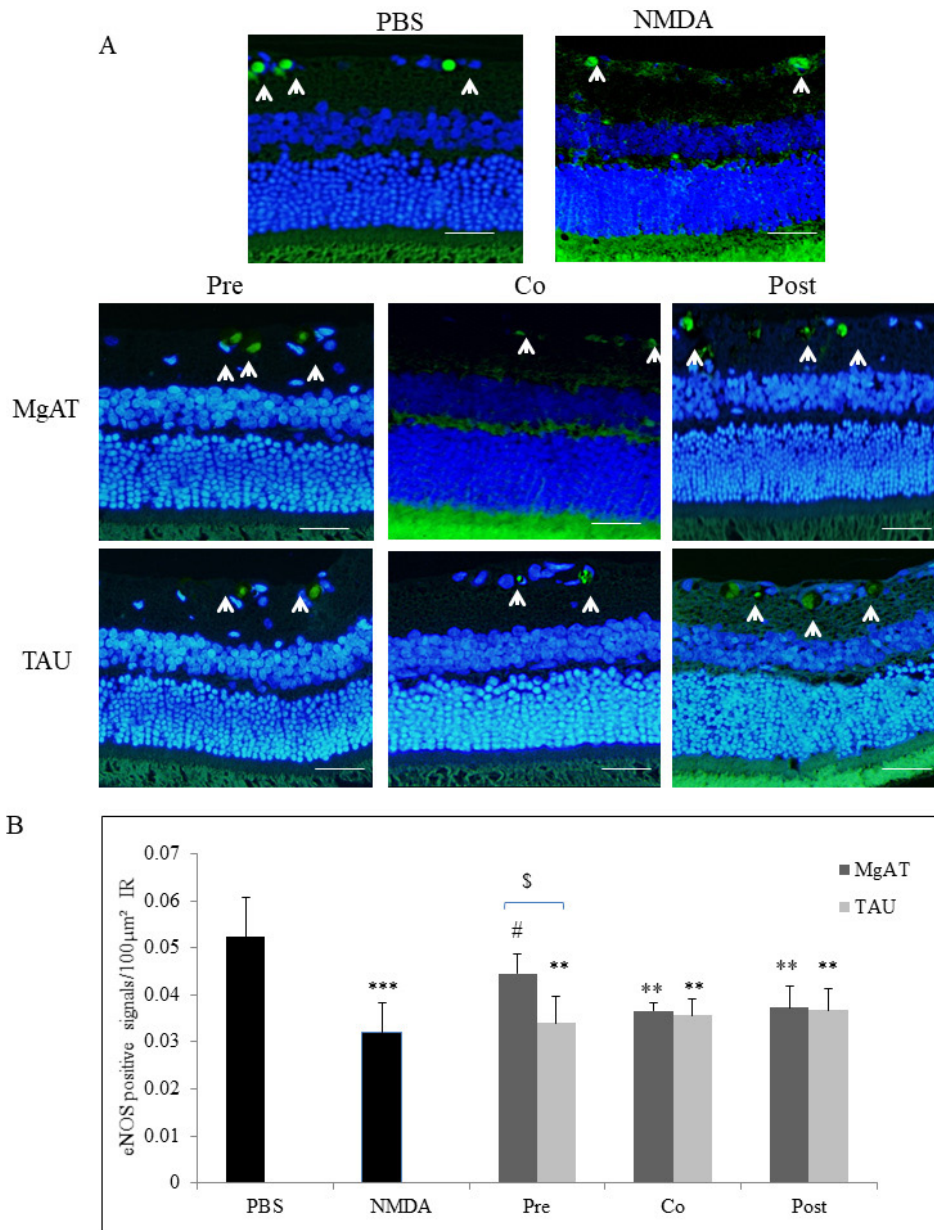


Figure 3. Effect of MgAT and TAU on NMDA-induced changes in eNOS expression. **A:** Microphotographs of retinal sections immunostained with eNOS antibodies showing the effect of MgAT and TAU on the NMDA-induced decrease in the expression of iNOS (20X). Green fluorescence shows eNOS expression stained with FITC (shown by arrow) while blue fluorescence shows retinal nuclei stained with 4',6-diamidino-2-phenylindole (DAPI). Scale bar represents 50 μm . **B:** Quantitative estimation of the effect of MgAT and TAU on the NMDA-induced decrease in the expression of eNOS is also represented graphically. Pre, Co, and Post indicate that MgAT/TAU were injected 24 h before, simultaneously, or 24 h after intravitreal administration of NMDA, respectively. ** $p < 0.01$ versus the PBS-treated group, *** $p < 0.001$ versus the PBS-treated group, # $p < 0.05$ versus the NMDA-treated group, \$ $p < 0.05$ corresponding MgAT versus TAU groups, $n = 6$; bars represent mean \pm SD. NMDA: N-methyl-D-aspartic acid, MgAT: Magnesium acetyl taurate, TAU: Taurine, GCL: Ganglion cell layer.

TABLE 1. EFFECT OF TREATMENT WITH MGAT AND TAU ON NMDA-INDUCED CHANGES IN RETINAL EXPRESSION OF NOS ISOFORMS AS DETERMINED BY ELISA.

Treatment		nNOS (ng/mg protein)	iNOS (ng/mg protein)	eNOS (pg/mg protein)
PBS		0.034±0.018	0.072±0.029	5.320±0.905
NMDA		4.729±0.880***	8.039±2.125***	1.926±0.980**
Pre	MgAT	0.422±0.179*##	0.247±0.108*##\$\$	3.789±0.214#\$
	Tau	0.513±0.178***##	1.659±0.521***##	2.536±0.492
Co	MgAT	0.558±0.196*#	1.498±0.369***##	3.162±0.639*#
	Tau	0.441±0.065***#	2.161±0.266***##	2.869±0.650*
Post	MgAT	2.952±0.956*	1.235±0.487*#	2.819±0.298*
	Tau	4.467±1.439**	1.950±0.587***#	2.783±0.623*

All values are mean ± SD n=6. *p<0.05 versus PBS group; **p<0.01 versus PBS group, ***p<0.001 versus PBS group, #p<0.05 versus NMDA group, ##p<0.01 versus NMDA group, \$p<0.05 corresponding MgAT versus TAU groups; \$\$p<0.01 corresponding MgAT versus TAU groups NMDA: N-methyl-D-aspartic acid, MgAT: Magnesium Acetyltaurate, TAU: Taurine, Pre: Treatment was given 24 h before NMDA; Co-treatment was co-administered with NMDA; Post: treatment was administered 24 h after NMDA.

groups, the fraction of the GCL thickness was 38.14±4.330 and 30.82±4.150, respectively. In both groups, the GCL thickness was significantly greater than in the NMDA-treated group (p<0.001 and p<0.05, respectively) but comparable to that in the PBS-treated group. Similarly, in the TAU pre- and cotreatment groups, the fraction of the GCL thickness within the IR was significantly greater than in the NMDA-treated groups (p<0.001 and p<0.05, respectively) with mean values of 30.90±4.67 and 30.66±4.61, respectively. We noted that the GCL thickness in the MgAT-pretreated group was significantly greater than that in the TAU-pretreated group (p<0.05). The MgAT and TAU post-treatment groups showed no significant difference in the GCL thickness compared to the NMDA-treated and PBS-treated groups with mean values of 27.96±3.390 and 25.89±3.740, respectively (Figure 4 and Figure 5A).

In accordance with the observations for the GCL thickness, we observed a 2.04-fold reduction in the number of retinal cell nuclei/100 µm² of the IR in the NMDA-treated group compared to the PBS-treated group with mean values

of 0.045±0.012 and 0.092±0.015, respectively (p<0.001). In the MgAT pre-, co-, and post-treatment groups, the number of retinal cell nuclei/100 µm² of the IR was increased by 2.35-, 2.38-, and 2.33-fold compared to the NMDA-treated group (p<0.001 for all three groups compared to the NMDA-treated group). The number of retinal cell nuclei/100 µm² of the IR showed an increase by 2.26-, 2.69-, and 2.25-fold in the TAU pre-, co-, and post-treatment groups, respectively, compared to the NMDA-treated group (p<0.001 for all three groups; Figure 4 and Figure 5B).

Effect of MgAT and TAU on NMDA-induced retinal cell apoptosis: The effect of MgAT and TAU against NMDA-induced retinal cell apoptosis was investigated using TUNEL staining, and the number of TUNEL-positive cells was expressed per 100 µm² of the IR. Although numerous apoptotic cells were visualized in the NMDA-treated group (0.038±0.005), a significantly lower number of apoptotic cells was seen in the PBS-treated group (0.018±0.005). Apoptotic signals were significantly fewer in the MgAT pre- and cotreatment groups (0.016±0.002 and 0.024±0.005, respectively) compared to the

TABLE 2. EFFECT OF MGAT AND TAU ON NMDA INDUCED RETINAL NITROSATIVE STRESS.

3-NT (ng/ml/ mg retina)	PBS	NMDA	PRE	CO	POST
				MgAT	
	0.703±0.171	1.133±0.081***	0.770±0.068###\$\$	0.954±0.127	0.979±0.106
				TAU	
			1.059±0.054**	1.042±0.079	1.071±0.071

Pre, Co and Post indicate that MgAT/TAU was injected 24 h before, simultaneously or 24 h after intravitreal NMDA administration, respectively. NMDA: N-methyl-D-aspartic acid, MgAT: Magnesium Acetyltaurate, TAU: Taurine **p<0.01 versus PBS group, ***p<0.001 versus PBS group, ###p<0.001 versus NMDA group, \$\$\$p<0.001 corresponding MgAT versus TAU groups

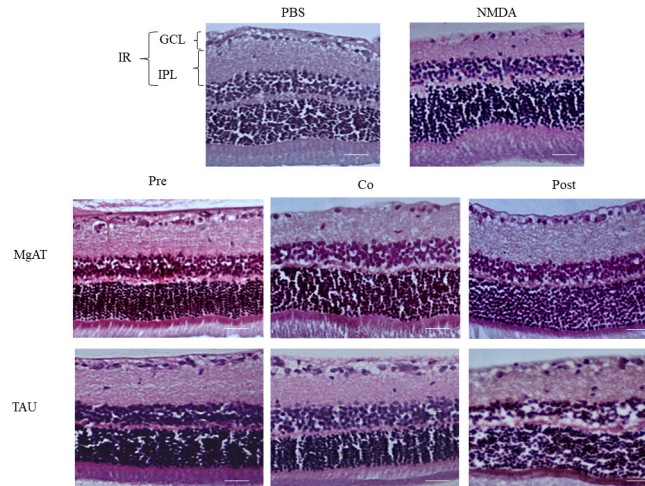


Figure 4. Effect of MgAT and TAU on NMDA-induced changes on retinal morphology (20X). Pre, Co, and Post indicate that MgAT/TAU were injected 24 h before, simultaneously, or 24 h after intravitreal administration of NMDA, respectively. Scale bar represents 50 μ m. NMDA: N-methyl-D-aspartic acid, MgAT: Magnesium acetyl taurate, TAU: Taurine, GCL: Ganglion cell layer, IPL: Inner plexiform layer; IR: Inner retina.

NMDA-treated group ($p < 0.001$ for both groups). The TAU pre- and cotreatment groups showed a significantly lower mean apoptotic cell count compared to the NMDA-treated group with mean values of 0.027 ± 0.002 ($p < 0.001$) and 0.029 ± 0.007 ($p < 0.05$), respectively. In both groups, however, the number of apoptotic cells was greater than in the PBS-treated group ($p < 0.05$ and $p < 0.001$, respectively). The extent

of apoptosis in the MgAT and TAU post-treatment groups (0.038 ± 0.003 and 0.033 ± 0.004 , respectively) was comparable to that in the NMDA-treated group. Among all groups, the MgAT pretreatment group showed the lowest number of apoptotic signals, and the apoptotic signal count in this group was significantly lower than that in the TAU pretreatment group ($p < 0.01$; Figure 6A,B).

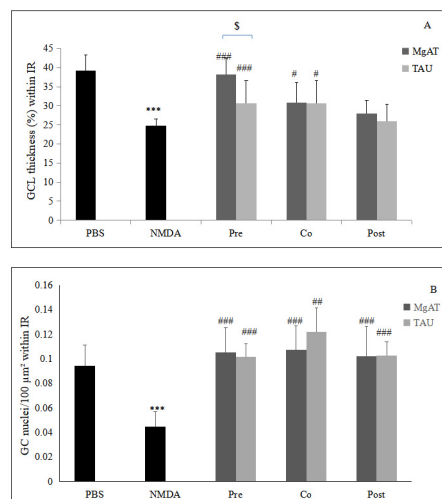


Figure 5. Quantitative estimation of the effect of MgAT and TAU on NMDA-induced changes in retinal morphology. Upper panel shows the effect of MgAT and TAU on NMDA-induced changes in the thickness of the GCL (%) within IR while the lower panel shows the effects of same on numeric density of the retinal cell nuclei in IR. Pre, Co, and Post indicate that MgAT/TAU were injected 24 h before, simultaneously, or 24 h after intravitreal administration of NMDA, respectively. NMDA: N-methyl-D-aspartic acid; MgAT: Magnesium

acetyltaurate; TAU: Taurine; GCL: Ganglion cell layer; IR: Inner retina *** $p < 0.001$ versus the PBS-treated group; # $p < 0.05$ versus the NMDA-treated group; ## $p < 0.01$ versus the NMDA-treated group; ### $p < 0.001$ versus the NMDA-treated group; \$ $p = 0.045$ corresponding MgAT versus TAU groups, N=6; Bars represent mean \pm SD.

In contrast to observations for nNOS, we observed reduced expression of eNOS in response to injection of NMDA despite its known Ca^{2+} -dependent expression. This result could be attributed to loss of endothelial cells in the retinal vessels after the NMDA injection. Ueda et al. showed that 7 days after a single intravitreal injection of NMDA, loss of RGCs and thinning of the inner plexiform layer are associated with the disappearance of endothelial cells, regression of vessels, and the presence of empty basement membrane sleeves [45]. In another study, endothelium-dependent vasodilation in retinal blood vessels was impaired 14 days after intravitreal injection of NMDA in rats [46]. Thus, NMDA-induced endothelial cell damage in retinal vessels seems to underlie reduced eNOS expression in NMDA-treated rat eyes. In a previous study, oral supplementation with magnesium N-acetyl taurate was shown to restore endothelial functions and endothelium-dependent vasodilation in Mg-deficient rats [47]. In accordance with these observations, in the present study, treatment with MgAT restored eNOS expression. We also observed significantly greater eNOS expression in eyes treated with TAU alone, which was in accordance with other studies that showed treatment with TAU improves endothelial function [48,49]. The extent of the increase in eNOS expression in all three TAU treated groups, however, remained lower compared to that in the corresponding MgAT-treated groups. This difference may perhaps be due to only a single dose of TAU in this study in contrast to the longer treatment duration in previous studies.

Excitotoxicity caused by NMDA in the present study was associated with significantly greater iNOS expression. iNOS is induced under pathological conditions, such as inflammation or ischemia. Activation of the NMDA receptor also results in increased expression of inflammatory cytokines; however, the mechanisms involved remain unclear. Moreover, NMDA-induced neuronal death mediated through cytokines depends on iNOS expression [50]. Increased iNOS activity generates a large amount of NO in a Ca^{2+} -independent manner [51]. Accordingly, in the present study we observed increased iNOS expression and increased 3-NT levels in response to exposure to NMDA. MgAT and TAU suppressed the NMDA-induced increase in iNOS expression. This effect of MgAT and TAU could be attributed to the antagonistic effect of magnesium and TAU on NMDA receptors [44,52]. Magnesium and TAU have previously been shown to suppress iNOS expression [53-55].

The present study did not include a treatment group with Mg alone because Mg has to be administered as a salt with

an anion such as MgCl_2 or MgSO_4 , and the anions affect the membrane permeation properties of Mg differently [56-60]. nNOS and iNOS are potent sources of NO generation [61], and as NMDA-induced expression of iNOS and eNOS was suppressed to a greater extent in the MgAT treatment group than TAU alone, we observed greater suppression of NO generation in the MgAT-treated group. Accordingly, the relative excess of retinal NO levels in the TAU-treated group led to greater retinal cell apoptosis and morphological alterations as observed in the TUNEL and H&E-stained retinal sections. Therefore, the difference in the GCL thickness and the extent of apoptosis between these two groups was significant ($p < 0.05$ and $p < 0.01$, respectively). A combined salt of Mg and TAU seems to produce greater efficacy in restoring NOS expression compared to TAU alone. In the TAU-treated groups, although significantly greater improvement was observed when we counted cells per $100 \mu\text{m}^2$ area of the IR, this could not be interpreted as near equal cell survival as seen in the corresponding MgAT-treated groups. As the cell count took into account the area of the IR, the cell count may show an apparent increase in the TAU group due to thinning of the GCL.

Importantly, we also observed that pretreatment with both MgAT and TAU produces greater reduction in retinal nitrosative stress compared to co- and post-treatment. It is likely that the pathological chain of events set up by exposure to NMDA to some extent overwhelms the protective effects of simultaneous or subsequent administration of MgAT and TAU. However, when pretreatment was given, MgAT and TAU interfered with excitotoxicity and subsequent events.

In conclusion, MgAT and TAU protect against NMDA-induced retinal cell apoptosis by preventing altered expression of all three types of NOS isoforms and thus, reduce retinal nitrosative stress. Pretreatment with MgAT and TAU is more effective in correcting NMDA-induced retinal nitrosative stress compared to co- and post-treatment. Additionally, the addition of Mg to TAU seems to enhance the benefits of TAU alone.

ACKNOWLEDGMENTS

We acknowledge the administrative and facility support by Research Management Institute, Institute of Medical Molecular Biotechnology (IMMB) and Laboratory Animal Care Unit, Universiti Teknologi MARA, Malaysia. Authors acknowledge the financial support by Universiti Teknologi MARA under grant no. 600-IRMI/DANA 5/3/BESTARI (006/2017) and 600-IRMI/DANA 5/3/LESTARI (0081/2016).

REFERENCES

1. Agarwal R, Gupta SK, Agarwal P, Saxena R, Agrawal SS. Current concepts in the pathophysiology of glaucoma. *Indian J Ophthalmol* 2009; 57:257-66. [PMID: 19574692].
2. Kwon YH, Rickman DW, Baruah S, Zimmerman MB, Kim CS, Boldt HC, Russell SR, Hayreh SS. Vitreous and retinal amino acid concentrations in experimental central retinal artery occlusion in the primate. *Eye (Lond)* 2005; 19:455-63. [PMID: 15184939].
3. Salt TE, Cordeiro MF. Glutamate excitotoxicity in glaucoma: throwing the baby out with the bathwater? *Eye (Lond)* 2006; 20:730-1. [PMID: 15951750].
4. Casson RJ. Possible role of excitotoxicity in the pathogenesis of glaucoma. *Clin Experiment Ophthalmol* 2006; 34:54-63. [PMID: 16451260].
5. Trump BF, Berezsky IK. Calcium-mediated cell injury and cell death. *FASEB J* 1995; 9:219-28. [PMID: 7781924].
6. Tymianski M, Charlton MP, Carlen PL, Tator CH. Source specificity of early calcium neurotoxicity in cultured embryonic spinal neurons. *J Neurosci* 1993; 13:2085-104. [PMID: 8097530].
7. Rameau GA, Chiu LY, Ziff EB. NMDA receptor regulation of nNOS phosphorylation and induction of neuron death. *Neurobiol Aging* 2003; 24:1123-33. [PMID: 14643384].
8. Fleming I. Molecular mechanisms underlying the activation of eNOS. *Pflugers Arch* 2010; 459:793-806. [PMID: 20012875].
9. Lv B, Huo F, Dang X, Xu Z, Chen T, Zhang T, Yang X. Puerarin Attenuates N-Methyl-D-aspartic Acid-induced Apoptosis and Retinal Ganglion Cell Damage Through the JNK/p38 MAPK Pathway. *J Glaucoma* 2016; 25:e792-801. [PMID: 27552519].
10. Nomura Y, Kitamura Y. Inducible nitric oxide synthase in glial cells. *Neurosci Res* 1993; 18:103-7. [PMID: 7510374].
11. Bonfoco E, Krainc D, Ankarcrona M, Nicotera P, Lipton SA. Apoptosis and necrosis: two distinct events induced, respectively, by mild and intense insults with N-methyl-D-aspartate or nitric oxide/superoxide in cortical cell cultures. *Proc Natl Acad Sci USA* 1995; 92:7162-6. [PMID: 7638161].
12. Dawson VL, Dawson TM, London ED, Brecht DS, Snyder SH. Nitric oxide mediates glutamate neurotoxicity in primary cortical cultures. *Proc Natl Acad Sci USA* 1991; 88:6368-71. [PMID: 1648740].
13. Neufeld AH, Hernandez MR, Gonzalez M. Nitric oxide synthase in the human glaucomatous optic nerve head. *Arch Ophthalmol* 1997; 115:497-503. [PMID: 9109759].
14. Agarwal R, Agarwal P. Rodent models of glaucoma and their applicability for drug discovery. *Expert Opin Drug Discov* 2017; 12:261-70. [PMID: 28075618].
15. Kwong JM, Lam TT. N-methyl-D-aspartate (NMDA) induced apoptosis in adult rabbit retinas. *Exp Eye Res* 2000; 71:437-44. [PMID: 10995563].
16. Siliprandi R, Canella R, Carmignoto G, Schiavo N, Zanellato A, Zanoni R, Vantini G. N-methyl-D-aspartate-induced neurotoxicity in the adult rat retina. *Vis Neurosci* 1992; 8:567-73. [PMID: 1586655].
17. Lam TT, Abler AS, Kwong JM, Tso MO. N-methyl-D-aspartate (NMDA)-induced apoptosis in rat retina. *Invest Ophthalmol Vis Sci* 1999; 40:2391-7. [PMID: 10476807].
18. Sakamoto K, Endo K, Suzuki T, Fujimura K, Kurauchi Y, Mori A, Nakahara T, Ishii K. P2X7 receptor antagonists protect against N-methyl-D-aspartic acid-induced neuronal injury in the rat retina. *Eur J Pharmacol* 2015; 756:52-8. [PMID: 25796199].
19. Kuroki T, Mori A, Nakahara T, Sakamoto K, Ishii K. Histological protection by nilvadipine against neurotoxicity induced by NOC12, a nitric oxide donor, in the rat retina. *Biol Pharm Bull* 2014; 37:306-10. [PMID: 24492726].
20. Sun Q, Ooi VE, Chan SO. N-methyl-D-aspartate-induced excitotoxicity in adult rat retina is antagonized by single systemic injection of MK-801. *Exp Brain Res* 2001; 138:37-45. [PMID: 11374081].
21. Marret S, Gressens P, Gadisseux JF, Evrard P. Prevention by magnesium of excitotoxic neuronal death in the developing brain: an animal model for clinical intervention studies. *Dev Med Child Neurol* 1995; 37:473-84. [PMID: 7789657].
22. Howard AB, Alexander RW, Taylor WR. Effects of magnesium on nitric oxide synthase activity in endothelial cells. *Am J Physiol* 1995; 269:C612-8. [PMID: 7573390].
23. Sun X, Mei Y, Tong E. Effect of magnesium on nitric oxide synthase of neurons in cortex during early period of cerebral ischemia. *J Tongji Med Univ* 2000; 20:13-5. [PMID: 12845745].
24. Chan CY, Sun HS, Shah SM, Agovic MS, Friedman E, Banerjee SP. Modes of direct modulation by taurine of the glutamate NMDA receptor in rat cortex. *Eur J Pharmacol* 2014; 728:167-75. [PMID: 24485893].
25. Hilgier W, Anderzhanova E, Oja SS, Saransaari P, Albrecht J. Taurine reduces ammonia- and N-methyl-D-aspartate-induced accumulation of cyclic GMP and hydroxyl radicals in microdialysates of the rat striatum. *Eur J Pharmacol* 2003; 468:21-5. [PMID: 12729839].
26. Tang XW, Deupree DL, Sun Y, Wu JY. Biphasic effect of taurine on excitatory amino acid-induced neurotoxicity. *Adv Exp Med Biol* 1996; 403:499-505. [PMID: 8915388].
27. El Idrissi A, Trenkner E. Growth factors and taurine protect against excitotoxicity by stabilizing calcium homeostasis and energy metabolism. *J Neurosci* 1999; 19:9459-68. [PMID: 10531449].
28. Chen WQ, Jin H, Nguyen M, Carr J, Lee YJ, Hsu CC, Faiman MD, Schloss JV, Wu JY. Role of taurine in regulation of intracellular calcium level and neuroprotective function in cultured neurons. *J Neurosci Res* 2001; 66:612-9. [PMID: 11746381].
29. Askwith T, Zeng W, Eggo MC, Stevens MJ. Taurine reduces nitrosative stress and nitric oxide synthase expression in high

- glucose-exposed human Schwann cells. *Exp Neurol* 2012; 233:154-62. [PMID: 21952043].
30. Liu Y, Tonna-DeMasi M, Park E, Schuller-Levis G, Quinn MR. Taurine chloramine inhibits production of nitric oxide and prostaglandin E2 in activated C6 glioma cells by suppressing inducible nitric oxide synthase and cyclooxygenase-2 expression. *Brain Res Mol Brain Res* 1998; 59:189-95. [PMID: 9729377].
 31. Aruoma OI, Halliwell B, Hoey BM, Butler J. The antioxidant action of taurine, hypotaurine and their metabolic precursors. *Biochem J* 1988; 256:251-5. [PMID: 2851980].
 32. Gaucher D, Arnault E, Husson Z, Froger N, Dubus E, Gondouin P, Dherbécourt D, Degardin J, Simonutti M, Fouquet S, Benahmed MA, Elbayed K, Namer IJ, Massin P, Sahel JA, Picaud S. Taurine deficiency damages retinal neurones: cone photoreceptors and retinal ganglion cells. *Amino Acids* 2012; 43:1979-93. Epub 2012 Apr 4 [PMID: 22476345].
 33. Shimada C, Tanaka S, Hasegawa M, Kuroda S, Isaka K, Sano M, Araki H. Beneficial effect of intravenous taurine infusion on electroretinographic disorder in taurine deficient rats. *Jpn J Pharmacol* 1992; 59:43-50. [PMID: 1507656].
 34. Arfuzir NN, Lambuk L, Jafri AJ, Agarwal R, Iezhitsa I, Sidek S, Agarwal P, Bakar NS, Kutty MK, Yusof AP, Krasilnikova A, Spasov A, Ozerov A, Mohd Ismail N. Protective effect of magnesium acetyltaurate against endothelin-induced retinal and optic nerve injury. *Neuroscience* 2016; 325:153-64. [PMID: 27012609].
 35. Lambuk L, Jafri AJ, Arfuzir NN, Iezhitsa I, Agarwal R, Rozali KN, Agarwal P, Bakar NS, Kutty MK, Yusof AP, Krasilnikova A, Spasov A, Ozerov A, Ismail NM. Neuroprotective Effect of Magnesium Acetyltaurate Against NMDA-Induced Excitotoxicity in Rat Retina. *Neurotox Res* 2017; 31:31-45. [PMID: 27568334].
 36. Agarwal R, Iezhitsa I, Awaludin NA, Ahmad Fisol NF, Bakar NS, Agarwal P, Abdul Rahman TH, Spasov A, Ozerov A, Mohamed Ahmed Salama MS, Mohd Ismail N. Effects of magnesium taurate on the onset and progression of galactose-induced experimental cataract: in vivo and in vitro evaluation. *Exp Eye Res* 2013; 110:35-43. [PMID: 23428743].
 37. Jafri AJ, Arfuzir NNN, Lambuk L, Iezhitsa I, Agarwal R, Agarwal P, Razali N, Krasilnikova A, Kharitonova M, Demidov V, Serebryansky E, Skalny A, Spasov A, Yusof APM, Ismail NM. Protective effect of magnesium acetyltaurate against NMDA-induced retinal damage involves restoration of minerals and trace elements homeostasis. *J Trace Elem Med Biol* 2017; 39:147-54. [PMID: 27908408].
 38. Takahata K, Katsuki H, Kume T, Ito K, Tochikawa Y, Muraoka S, Yoneda F, Kashii S, Honda Y, Akaike A. Retinal neurotoxicity of nitric oxide donors with different half-life of nitric oxide release: involvement of N-methyl-D-aspartate receptor. *J Pharmacol Sci* 2003; 92:428-32. [PMID: 12939529].
 39. Razali N, Agarwal R, Agarwal P, Kapitonova MY, Kannan Kutty M, Smirnov A, Salmah Bakar N, Ismail NM. Anterior and posterior segment changes in rat eyes with chronic steroid administration and their responsiveness to antiglaucoma drugs. *Eur J Pharmacol* 2015; 749:73-80. [PMID: 25481859].
 40. Razali N, Agarwal R, Agarwal P, Tripathy M, Kapitonova MY, Kutty MK, Smirnov A, Khalid Z, Ismail NM. Topical trans-resveratrol ameliorates steroid-induced anterior and posterior segment changes in rats. *Exp Eye Res* 2016; 143:9-16. [PMID: 26424219].
 41. Parathath SR, Parathath S, Tsirka SE. Nitric oxide mediates neurodegeneration and breakdown of the blood-brain barrier in tPA-dependent excitotoxic injury in mice. *J Cell Sci* 2006; 119:339-49. [PMID: 16410551].
 42. Morgan J, Caprioli J, Koseki Y. Nitric oxide mediates excitotoxic and anoxic damage in rat retinal ganglion cells cocultured with astroglia. *Arch Ophthalmol* 1999; 117:1524-9. [PMID: 10565522].
 43. Pacher P, Beckman JS, Liaudet L. Nitric oxide and peroxynitrite in health and disease. *Physiol Rev* 2007; 87:315-424. [PMID: 17237348].
 44. Chan CY, Singh I, Magnuson H, Zohaib M, Bakshi KP, Le François B, Anazco-Ayala A, Lee EJ, Tom A, YeeMon K, Ragnauth A, Friedman E, Banerjee SP. Taurine Targets the GluN2b-Containing NMDA Receptor Subtype. *Adv Exp Med Biol* 2015; 803:531-44. [PMID: 25833525].
 45. Ueda K, Nakahara T, Hoshino M, Mori A, Sakamoto K, Ishii K. Retinal blood vessels are damaged in a rat model of NMDA-induced retinal degeneration. *Neurosci Lett* 2010; 485:55-9. [PMID: 20801189].
 46. Mori A, Hanada M, Sakamoto K, Nakahara T, Ishii K. Impaired retinal vasodilator response to acetylcholine in a rat model of NMDA-induced retinal degeneration. *J Pharmacol Sci* 2015; 127:211-6. [PMID: 25727959].
 47. Kharitonova M, Iezhitsa I, Zheltova A, Ozerov A, Spasov A, Skalny A. Comparative angioprotective effects of magnesium compounds. *J Trace Elem Med Biol* 2015; 29:227-34. [PMID: 25127069].
 48. Fennessy FM, Moneley DS, Wang JH, Kelly CJ, Bouchier-Hayes DJ. Taurine and vitamin C modify monocyte and endothelial dysfunction in young smokers. *Circulation* 2003; 107:410-5. [PMID: 12551864].
 49. Dalaklioglu S, Kuscü N, Celik-Ozenci C, Bayram Z, Nacitarhan C, Ozdem SS. Chronic treatment with taurine ameliorates diabetes-induced dysfunction of nitric oxide-mediated neurogenic and endothelium-dependent corpus cavernosum relaxation in rats. *Fundam Clin Pharmacol* 2014; 28:394-404. [PMID: 23848484].
 50. Hewett SJ, Csernansky CA, Choi DW. Selective potentiation of NMDA-induced neuronal injury following induction of astrocytic iNOS. *Neuron* 1994; 13:487-94. [PMID: 7520256].
 51. Becquet F, Courtois Y, Goureau O. Nitric oxide in the eye: multifaceted roles and diverse outcomes. *Surv Ophthalmol* 1997; 42:71-82. [PMID: 9265703].
 52. Decollogne S, Tomas A, Lecerf C, Adamowicz E, Seman M. NMDA receptor complex blockade by oral administration of

- magnesium: comparison with MK-801. *Pharmacol Biochem Behav* 1997; 58:261-8. [PMID: 9264101].
53. Luo WB, Dong L, Wang YP. Effect of magnesium lithospermate B on calcium and nitric oxide in endothelial cells upon hypoxia/reoxygenation. *Acta Pharmacol Sin* 2002; 23:930-6. [PMID: 12370098].
 54. Zhao Z, Tang Z, Zhang W, Liu J, Li B. Magnesium isoglycyrrhizinate protects against renal-ischemia-reperfusion injury in a rat model via anti-inflammation, anti-oxidation and anti-apoptosis. *Mol Med Rep* 2017; 16:3627-33. [PMID: 28714024].
 55. Kato T, Tsunekawa M, Wang S, Yamashita T, Ma N. Effect of Taurine on iNOS-Mediated DNA Damage in Drug-Induced Renal Injury. *Adv Exp Med Biol* 2017; 975:717-27. [PMID: 28849494].
 56. Durlach J, Guiet-Bara A, Pagès N, Bac P, Bara M. Magnesium chloride or magnesium sulfate: a genuine question *Magnes Res* 2005; 18:187-92. [PMID: 16259379].
 57. Spasov AA, Petrov VI, Iezhitsa IN, Kravchenko MS, Kharitonova MV, Ozerov AA. Comparative study of magnesium salts bioavailability in rats fed a magnesium-deficient diet. *Vestn Ross Akad Med Nauk* 2010; 2:29-37. [PMID: 20364677].
 58. Spasov AA, Iezhitsa IN, Kravchenko MS, Kharitonova MV, Stukovina AY, Naumenko LV. Effect of oral organic and inorganic magnesium salts on hemorheological state of rats fed with magnesium-deficient diet. *Gematologiya i Transfusiologiya* 2007; 52:38-44. .
 59. Spasov AA, Ozerov AA, Iezhitsa IN, Kharitonova MV, Kravchenko MS, Zheltova AA. Correction of furosemide-induced magnesium deficiency with different stereoisomers of organic magnesium salts: a comparative study. *Bull Exp Biol Med* 2011; 151:333-5. [PMID: 22451880].
 60. Iezhitsa IN, Spasov AA, Zhuravleva NV, Sinolitskii MK, Voronin SP. Comparative study of the efficacy of potassium magnesium L-, D- and DL-aspartate stereoisomers in overcoming digoxin- and furosemide-induced potassium and magnesium depletions. *Magnes Res* 2004; 17:276-92. [PMID: 15726904].
 61. Thomas DD, Ridnour LA, Isenberg JS, Flores-Santana W, Switzer CH, Donzelli S, Hussain P, Vecoli C, Paolucci N, Ambs S, Colton CA, Harris CC, Roberts DD, Wink DA. The chemical biology of nitric oxide: implications in cellular signaling. *Free Radic Biol Med* 2008; 45:18-31. [PMID: 18439435].

Articles are provided courtesy of Emory University and the Zhongshan Ophthalmic Center, Sun Yat-sen University, P.R. China. The print version of this article was created on 25 July 2018. This reflects all typographical corrections and errata to the article through that date. Details of any changes may be found in the online version of the article.